ABUAD Journal of Engineering Research and Development (AJERD)
ISSN (online): 2645-2685; ISSN (print): 2756-6811

Volume 8, Issue 3, 1-11

Characterization and Comminution Energy Determination of Anka Manganese Ore for Steelmaking Applications

Yemisi Elizabeth GBADAMOSI, Oladunni Oyelola ALABI, Joseph Olatunde BORODE, Fatai Olufemi ARAMIDE

Metallurgical and Materials Engineering Department, School of Infrastructures, Minerals, and Manufacturing Engineering, Federal University of Technology Akure, P.M.B 704, Akure, Ondo State Nigeria
gbadamosiyemisi.e@gmail.com/aoalabi@futa.edu.ng/joborode@futa.edu.ng/foaramide@futa.edu.ng

Corresponding Author: gbadamosiyemisi.e@gmail.com, *+2347054710291*
Date Submitted: *04/07/2025*
Date Accepted: *08/09/2025*
Date Published: *09/09/2025*

Abstract: *The global demand for manganese continues to rise due to its critical role in steelmaking and emerging battery technologies. This study investigates the physicochemical properties and comminution energy requirements of manganese ore from the Anka deposit in Zamfara State, Nigeria. A comprehensive characterization was conducted using Energy Dispersive X-Ray Fluorescence (ED-XRFS), X-Ray Diffraction (XRD), and Scanning Electron Microscopy with Energy Dispersive Spectroscopy (SEM-EDS). Particle size analysis was carried out on the as-received sample, followed by a grindability test. The chemical analysis confirmed a high MnO content (52.112%), while mineralogical assessments identified pyrolusite and jacobsite as dominant phases. SEM-EDS analysis revealed the interlocking nature of manganese, iron, silicon, and aluminium within the ore matrix. Particle size analysis identified the optimal liberation size at -125+90 µm, assaying 53.973% MnO. Grindability tests using quartz and iron as reference ores yielded work index values of 11.34 kWh/ton and 14.62 kWh/ton, respectively. The average energy expended during grinding was 5.06 kWh. These findings provide a basis for designing energy-efficient beneficiation processes for Anka manganese ore, contributing to sustainable resource utilization and industrial cost reduction.*

Keywords: *Chemical Analysis, Mineralogical Characterization, Particle Size Analysis, Grindability Test, Anka Manganese*

1. INTRODUCTION

Manganese (Mn) is essential for enhancing the mechanical properties of steel, including strength, toughness, and wear resistance. It also plays a vital role in specialized alloys and battery technologies for electric vehicles and energy storage systems [1, 2, 3]. Manganese stands out as one of the crucial metals worldwide due to industrial expansion and technological innovation, coupled with the evolution of cleaner power systems, but it requires the efficient management of available assets found in distinct ore compositions [4, 5]. The mines estimates suggest that Nigeria's manganese reserves amount to approximately 140 million tons, presenting a substantial opportunity for both local and international investment in mining and beneficiation activities [6]. Nigeria possesses substantial manganese deposits, particularly in regions like Zamfara State, where the Anka deposit is located, presenting a potential opportunity for economic and industrial growth [7]. Anka mines is about 420 hectares of land mass between the geological coordinates of latitude 12°06′30″N and longitude 5°56′00″E. However, realizing the economic potential of these resources depends on a thorough understanding of the ore's fundamental properties and the energy required for its efficient and cost-effective processing, considering both economic and environmental sustainability [8]. Previous studies have explored manganese ore beneficiation, but few have quantified the comminution energy specific to Nigerian deposits. This study addresses that gap by characterizing the Anka manganese ore and determining its grindability using standardized method. The novelty lies in establishing the liberation size and energy profile of this deposit, which informs cost-effective beneficiation strategies and supports sustainable mining practices.

A set of analytical techniques constitutes characterization, which provides complete definitions of ore properties alongside its structural composition. The X-ray fluorescence (XRF) spectroscopy method analyses the elemental substances of the ore by identifying the percentage composition of the elements and compounds present. The elemental analysis of ores helps determine their quality and allows recognition of potential problems in downstream processing to select appropriate beneficiation approaches from conventional and innovative tactics [9, 10]. The identification of ore mineral phases through X-ray diffraction (XRD) analysis performs mineralogical characterization of the ore [11, 12]. Determining the mineral composition helps researchers create separation processes that enhance ore recovery while reducing other unwanted elements in the final products and enable the extraction of valuable products [13]. The scanning electron microscopy (SEM) with energy-dispersive spectroscopy (EDS) reveals details of the ore microtexture and element distribution within the ore matrix and shows the mineral relationship between the mineral of interest and non-valuable

minerals. Processing efficiency heavily depends on particle size analysis to determine the sieve fraction with significant liberation of the mineral of interest, which affects operational efficiency. Operational efficiency within crushing and grinding process circuits relies on the measurement of ore particle sizes obtained through sieving analysis [14, 15]. Evaluating the economic potential of manganese ore deposits requires a determination of the necessary comminution energy of the ore body [16, 17]. The energy requirement for grinding ore increases with its bond work index, which simultaneously drives up processing plant capital investment and operating expenses; therefore, energy-efficient comminution technologies must be examined. The measurement of comminution energy remains essential as it decides whether mining and processing a specific ore is financially viable and determines how to establish effective sustainable comminution procedures. The research seeks to evaluate the chemical and mineralogical composition of the ore for processing, alongside particle size examinations and grindability tests to achieve optimal comminution energy for cost-effective processing of Anka manganese ore.

1.1 Grindability Test – Work Index Determination

In the mineral industry, comminution is the highest consumer of energy. With the limited energy resources, the need to design energy requirements of engineering processes cannot be overemphasized. Grindability is the ability of a material to be made smaller by grinding. The bond standard grindability test provides a work index that is widely used to estimate the energy required for grinding [18]. The work index measures a material's resistance to crushing and grinding. It is defined as the kilowatt hours per ton needed to decrease the material from an infinitely large feed size to a size where 80% of it passes through 100 µm sieve. Work index is mathematically expressed as given in Equation 1.

$$W = \frac{10\,Wi}{\sqrt{P}} - \frac{10\,Wi}{\sqrt{F}} \quad (1)$$

W = Work Index
P = Diameter of the reference ore/ test ore through which 80% of the product passes through 100 µm (micron)
F = Diameter of the reference ore/ test ore through which 80% of the feed passes through 100 µm (micron)

To determine the precise sieve size at which 80% of the material passes, a known sieve size where close to 80% of the material passes is selected. The unknown sieve size is then computed using the Gaudin Schumman expression, which is mathematically expressed as given in Equation 2.

$$\text{Sieve } 1 = \frac{\%\,passing\ sieve\ 1}{\%\,passing\ seive\ 2} \times X \quad (2)$$

X = Sieve mesh size with 80% of particle size passing

2. MATERIALS AND METHOD

2.1 Materials

The manganese ore samples originated from the Anka district in Zamfara State of northwestern Nigeria. 10 kg of Anka manganese was collected from different pits across the Anka mines to achieve sample evenness and reduce analytical bias with quartz and iron (reference ore – Figure 1 – 2), the overburden layer used for the grindability test. Samples were crushed, pulverized and ground using the laboratory jaw crusher, pulverizer and ball mill machine.

Figure 1: Pulverized over burden Layer 1 (quartz)

Figure 2: Pulverized over burden Layer 2 (iron rich)

2.1.1 Analytical workflow

A schematic diagram summarizing the experimental workflow is presented in Figure 3**.**

2.2 Methods

2.2.1 Chemical characterization

Evaluation of Anka Manganese ore chemical composition using energy dispersive X-ray fluorescence spectrometry (ED-XRFS) technique. The scientific analysis was performed with the use of Xenemetric Genius 'IF' model ED-XRFS at the National Steel Raw Materials Exploration Agency, Kaduna. The laboratory ball mill used to reduce the ore samples to

a fine powder (-200 mesh) for both homogeneity purposes and reduction of particle size effects before analysis. The powdered ore material – 5g was charged into sample receptacles before conducting vacuum-based analyses. Software from the instrument processed the data to obtain quantitative measurement results

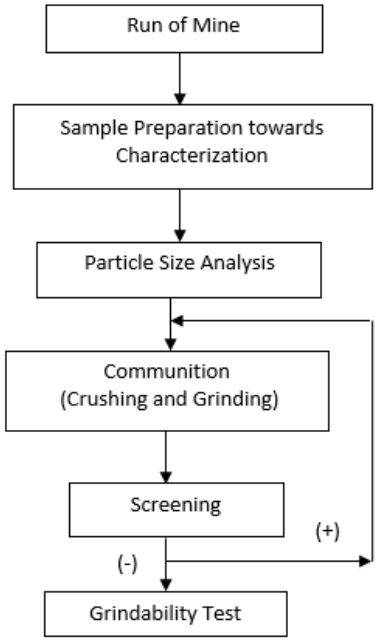

Figure 3: A schematic of the experimental workflow

2.2.2 Mineralogical characterization

i. **Mineral phase identification:** The XRD analysis identified the minerals present in the Anka manganese ore. An XRD analysis was performed using CuKα radiation in continuous scan operations by varying 2θ angles from 5° to 80°. The diffractogram reached its highest resolution after completing optimization of the step size alongside the scan rate. The adopted analysis software (X'Pert HighScore Plus) processed the diffractogram to determine which minerals existed in the ore sample.

ii. **Microstructural and elemental analysis:** A polished thin section of ore samples was prepared to examine the Anka manganese using the SEM-EDS (Phenom Pro 'X' model) at the National Steel Raw Materials Exploration Agency, Kaduna. The analysis was performed by mounting these samples onto stubs, followed by a carbon conductive layer for SEM exploitation. An assessment of surface features and compositional contrasts within the ore was done through secondary electron (SE) and backscattered electron (BSE) detectors in SEM analysis. The analysis tool EDS performed elemental assessments at the pre-selected points on the sample to reveal mineral grain compositions with their placement details. The instrument software processed obtained data to extract both quantitative and qualitative elemental results.

2.2.3 Particle size analysis

The sieves were properly cleaned to prevent contamination of the sample and arranged in accordance to the √2 series, ranging from 1000 µm - 63 µm (micron) [19]. One hundred grams of the sample were taken and placed into the uppermost sieve. A tightly fitting pan was positioned below the bottom sieve to collect the final undersize, and a lid was placed on top of the coarsest sieve to prevent the escape of the sample. The set of sieves was placed on the automated Denver sieve shaker and agitated for 15 minutes, during the vibration, the undersize material falls through successive sieves until it is retained on a sieve having apertures which were slightly smaller than the diameter of the particle [19]. The set of sieves was separated and the particles retained on each of the sieves were weighed using the Dawood digital weighing balance model DA3002, sieve analysis table was tabulated. The sieve fractions were chemically characterized via ED-XRFS to determine the economic liberation size of the Anka manganese ore.

2.2.4 Grindability test

The grindability test of the Anka manganese ore was computed using the Gaudin Schumann expression and the modified Bond's equation. The test ore – Anka manganese has two overburden layers of known work index values. A representative sample of Anka manganese ore, quartz and iron was broken with a sledge hammer to provide required size acceptable as feed to the Fritsch Pulveristte laboratory pulverizer. 100 g each of the test and reference samples from the laboratory pulverizer were then charged into the set of sieves which was placed on the automated Denver sieve shaker which vibrates the sieve in a vertical plane for 15 minutes and each sieve fraction retained of the test and reference ores

were weighed and the value noted as feed product into ball mill (Ft / Fr). 100 g each from pulverized samples was ground in the Denver laboratory ball mill machine size D-12 for 10 minutes and was also charged into the set of sieves which was placed on the automated Denver sieve shaker which vibrates the sieve in a vertical plane for 15 minutes and each sieve fraction retained of the test and reference ore were weighed and the value noted as product from ball mill (Pt/Pr).

3. RESULTS AND DISCUSSION

3.1 Chemical Composition of Anka Manganese Ore

The chemical content of Anka manganese ore was analyzed using the energy dispersive X-Ray fluorescence spectrometer (ED-XRFS), result is reported in Table 1. Chemical analysis shows that manganese oxide (MnO) is the main component assaying 52.112% of the total ore composition. The substantial MnO content classifies this deposit as an attractive mineral resource that finds applications in steelmaking operations [1, 2]. The mineral analysis revealed silicon dioxide present at 17.016% while aluminium dioxide existed at 15.297% in the ore composition. The identified metal oxides specifically demonstrate silicate gangue mineral behavior because they indicate that non-metallic impurities exist at high levels which will impact the beneficiation procedure. [9, 10] have independently proven silicate minerals as the primary challenge during manganese ore processing. Iron-bearing phases and iron oxide exist as 10.941% Fe_2O_3 in the ore. The minor oxide composition includes calcium oxide (CaO with 2.020%) and titanium dioxide (TiO_2 with 0.559%) and potassium oxide (K_2O with 0.273%) and phosphorus pentoxide (P_2O_5 with 0.410%). During steel beneficiation the steel industry requires reductions of phosphorus because high amounts lead to degraded steel quality. The analysis revealed minimal concentrations of transition metal oxides including V_2O_5 at 0.126% alongside NiO at 0.081% and CuO at 0.040%, ZnO at 0.085% along with Ta_2O_5 at 0.069%. Various trace amounts of elements exist at very low levels. The presence of chloride (Cl, 0.478%) and sulphate (SO_3, 0.223%) in the ore might affect its leaching behaviour while presenting environmental challenges during production and waste disposal.

Table 1: Chemical constituents of Anka Manganese Ore

Constituent	MnO	SiO_2	Al_2O_3	Fe_2O_3	CaO	TiO_2	Cl	P_2O_5	CuO
Comp. (%)	52.112	17.016	15.297	10.941	2.020	0.559	0.478	0.410	0.040

Constituent	K_2O	SO_3	BaO	V_2O_5	ZnO	NiO	Ta_2O_5	WO_3	Cr_2O_3
Comp. (%)	0.273	0.223	0.196	0.126	0.085	0.081	0.069	0.049	0.025

3.2 Phase Identification of Anka Manganese Ore

The X-ray diffraction (XRD) analysis determined the mineralogical content of Anka manganese ore as shown in Table 2 and Figure 4a – 4b. XRD analysis revealed the main phase of Anka manganese ore to be pyrolusite (MnO_2) with a figure of merit (FOM) 1.772. The identified manganese oxide mineral and principal extraction source of manganese match previous research findings by [11] and [12]. The identified phase confirms that the MnO compounds seen through elemental analysis existed in the sample. Figure of merit is a numerical parameter that helps determine how reliable and accurate the phase identification of a sample is, especially in complex mixtures where multiple phases exist. [23]. A figure of merit of 3.436 was observed for jacobsite ($MnFe_2O_4$) as a spinel-type oxide. Different mineral forms of manganese such as pyrolusite and jacobsite, co-occurrence in the ore affects both reducibility properties and possible beneficiation methods [13]. The FOM of quartz (SiO_2) was 1.266, which complements the significant silicate gangue present in the chemical analysis. The presence of quartz indicates the need for desilication during processing since the approach is considered widespread in manganese ore beneficiation operations [9]. The analysis also revealed corundum (Al_2O_3) with FOM 3.412, the high aluminium content obtained in the chemical analysis was confirmed, together with evidence of resistant alumino-silicate minerals in this phase analysis. The analysis revealed lime (CaO) as a synthetic phase with FOM of 3.345. The presence of lime in lower quantities indicates that either carbonate precursors or calcareous gangue might be present as impurities.

Table 2: Mineral phases detected in Anka Manganese Ore Sample via XRD

Phase name	**Formula**	**Figure of merit**
Pyrolusite	MnO_2	1.772
Jacobsite	$MnFe_2O_4$	3.436
Quartz	SiO_2	1.266
Corundum	Al_2O_3	3.412
Lime, syn	CaO	3.345

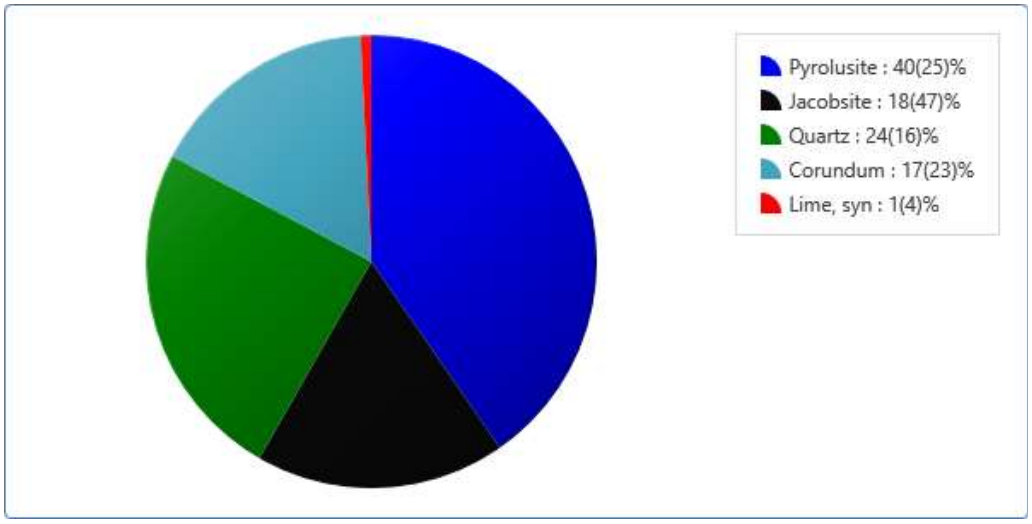

Figure 4a: Pie Chart representation of mineral phases present in Anka Manganese Ore

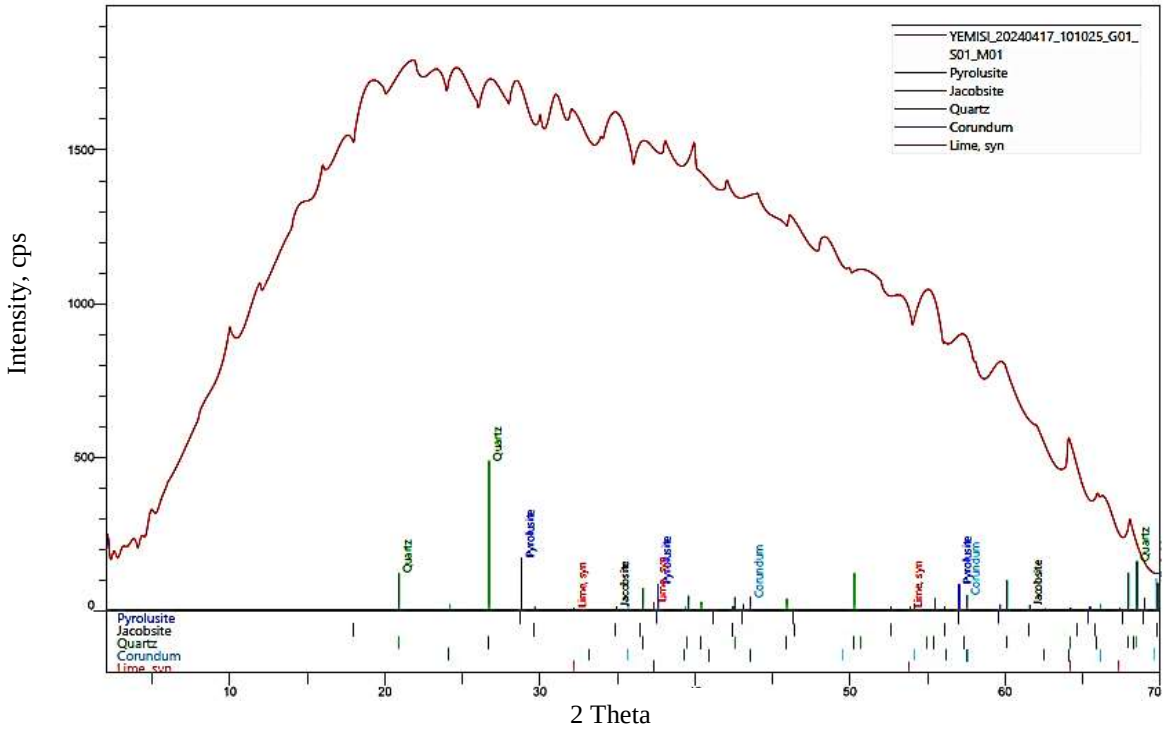

Figure 4b: Diffractogram of Anka Manganese Ore showing the mineral peaks

3.3 Microstructural Analysis of Anka Manganese Ore using SEM-EDS

The SEM micrograph (Figure 5) was obtained at a 500x magnification level demonstrates that the ore consists of numerous individual particles and larger clusters. The non-coherent shape of these particles indicates a poor development of euhedral crystal structures, and they likely formed because of fracturing and aggregative processes. Various mineral compositions are present in the ore, the observed particle dimension range demonstrates heterogeneity of its components. The ore mineral surface topography shows mainly rough structures. The EDS spectrum (Figure 6, Table 3) provides quantitative and qualitative data about the elemental substances in the Anka manganese ore. X-ray emission peaks show that manganese (Mn) and iron (Fe) stand as the main spectral components, the quantity of manganese indicating that the examined sample meets the definition of manganese ore while revealing high iron content. Other constituents in the sample matrix are silicon (Si) and aluminium (Al) since their notable peak intensities prove their substantial amounts. Potassium (K) and calcium (Ca) appear with moderate peak intensities, which points to their presence in smaller detectable amounts. The analysis showed sodium (Na), together with magnesium (Mg) and titanium (Ti), and Strontium (Sr) appear in trace quantities, which can be seen through their less intense peaks. The analysis indicates phosphorus (P), sulfur (S) and chlorine (Cl) show extremely weak peaks, indicating minimal occurrence, likely because they exist as trace materials. The

EDS spectrum results backed by SEM imaging of irregular mineral particles indicate that various manganese-iron oxide and hydroxide minerals exist in the ore. Moreover, the observed characteristics can be attributed to typical manganese ore minerals, including high-grade manganese dioxide (MnO_2) and manganite (MnO(OH)), along with iron-bearing phases consisting either of goethite (FeO(OH)) or hematite (Fe_2O_3). The substantial amounts of silicon and aluminium strongly support the presence of silicate-based gangue minerals. These minerals can include widespread quartz (SiO_2) together with feldspar minerals which are potassium, sodium and calcium aluminosilicates and also different clay minerals. The analysis of both potassium and calcium amounts strengthens the evidence that feldspar minerals exist considerably in the gangue material. The combination of various grain sizes shown in SEM images, together with EDS's different elemental findings, confirms the complex distribution of minerals within the Anka manganese ore. The detected trace elements exist either by occupying positions in the crystal structures of major mineral phases as major cation substitutions or as separate minor accessory mineral phases within the ore bulk [11, 20].

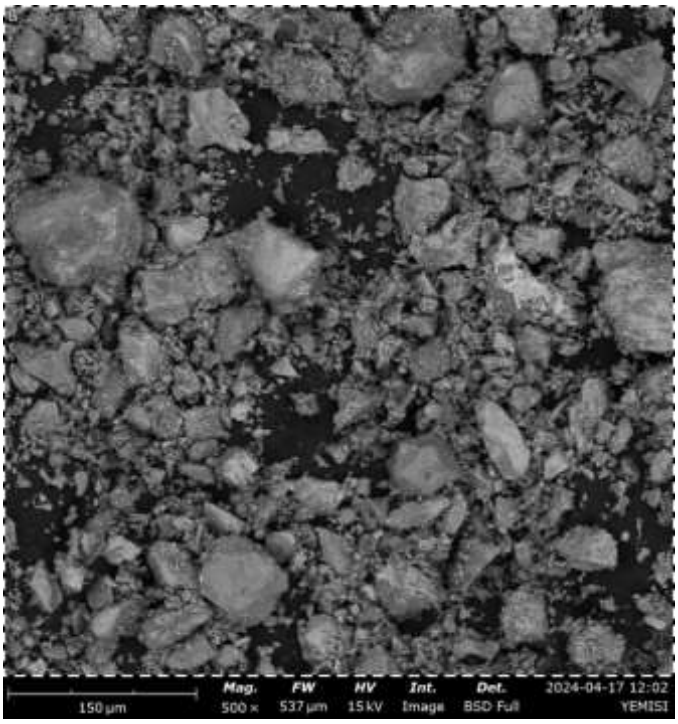

Figure 5: SEM micrograph of Anka Manganese Ore

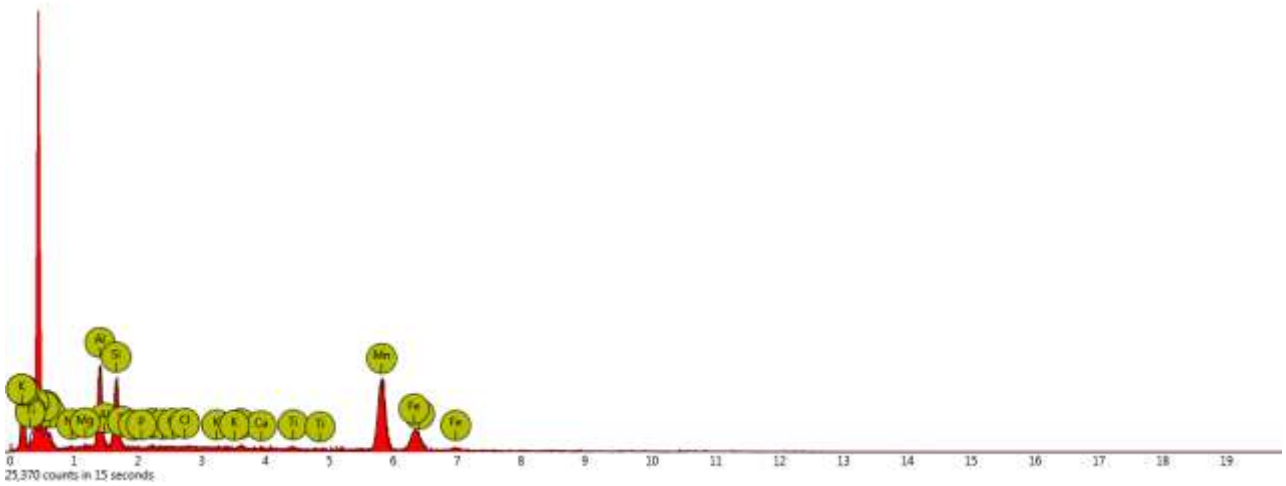

Figure 6: Energy dispersive spectrum (EDS) of Anka Manganese Ore

Table 3: Elemental composition of Anka Manganese Ore (EDS Analysis)

Element number	Element symbol	Atomic conc. (%)	Weight conc. (%)
25	Mn	45.33	57.20
26	Fe	11.91	15.27
13	Al	22.05	13.67
14	Si	18.25	11.77
22	Ti	0.86	0.95
20	Ca	0.61	0.56
11	Na	0.48	0.25
16	S	0.27	0.20
12	Mg	0.24	0.13

3.4 Chemical Constituents of Anka Manganese Ore Based on Particle Size Analysis

Particle size analysis of Anka manganese ore was carried out using the root 2 sieve size range and the result obtained was reported in Table 4 and Figure 7. The result shows that the highest weight percent of the ore retained in the largest particle sieve size (+1400 µm) which is 62.33%. The result shows that with reducing particle size, the weight percent retained reduces linearly except for a deviations in the -710+500 µm (9.61%) and -1400+1000 µm (7.15%) sieve sizes. The percentage of MnO across the sieve sizes showed fairly consistent concentration of 46.746 % to 53.973%. The relatively even distribution of MnO concentration across the sieve sizes is a typical feature found in geochemical analysis of manganese ores [11]. Significant liberation of mineral of interest was achieved at -125+90 µm assaying MnO concentration of 53.973%, indicating the actual liberation size of Anka manganese ore. The fairly consistent distribution of MnO across the different size fractions is an indication that the manganese mineralization is scattered throughout the ore body [14, 15].

Table 4: Result of the particle size analysis of Anka Manganese Ore

Sieve size range (µm)	Weight retained (g)	% Weight retained	% Cumulative weight retained	% Cumulative weight passing	% MnO
+1400	121.65	62.33	62.33	37.67	51.543
-1400+1000	13.96	7.15	69.48	30.52	47.238
-1000+710	8.44	4.32	73.80	26.20	51.522
-710+500	18.76	9.61	83.41	16.59	50.142
-500+355	8.05	4.12	87.53	12.47	46.798
-355+250	2.64	1.35	88.88	11.12	50.939
-250+180	1.85	0.94	89.82	10.18	49.746
-180+125	4.23	2.20	92.03	7.97	49.073
-125+90	5.30	2.71	94.74	5.26	53.973
-90+63	5.26	2.69	97.43	2.57	48.767
-63	5.02	2.57	100	0	52.180

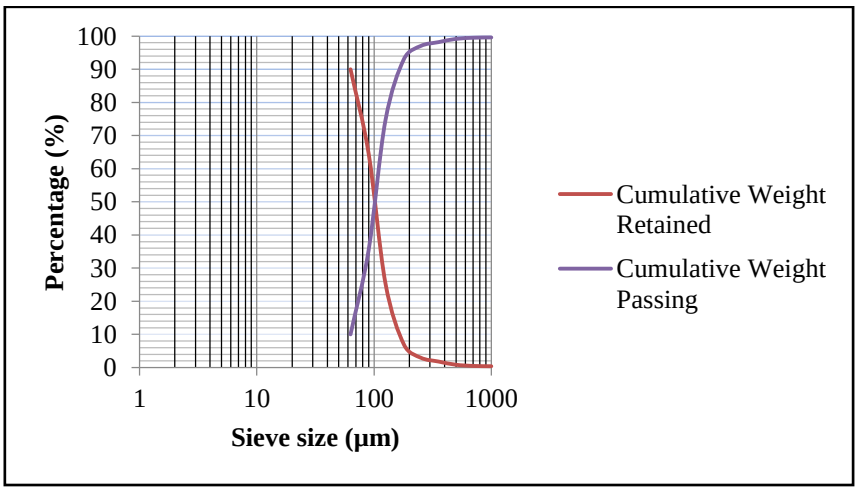

Figure 7: Plot of % cumulative weight retained and % cumulative weight passing against sieve sizes (µm)

3.5 Grindability Test – Work Index Determination

Table 5 – Table 10 present the sieve analysis result of the feed to ball mill and product out of ball mill for quartz (overburden layer 1), iron (overburden layer 2) and manganese ore (test ore). The obtained values from the sieve analysis was computed using the Gaudin Schumann Expression to determine the 80% passing of both the test ore and the two reference ores (Table 11). The obtained values was evaluated using the modified bond's equation to determine the Anka manganese work index and energy to be expended during grinding of the ore. The result of work index and energy expended during grinding is presented in Table 12. The work index Anka manganese ore with quartz as the overburden layer is calculated as 11.34 kWh/ton, and for iron as the overburden layer the work index is 14.62 kWh/ton. The difference between the work index values for the two overburden layers shows that the iron ore in the Anka manganese ore is more resistant to grinding than the quartz. The average work index of Anka manganese ore for both constituents is 12.98 kWh/ton. This gives an overall estimate of the grinding energy for this ore, establishing the energy expenditure involved in the comminution process. Energy expended during grinding with quartz as the overburden layer of the ore requires 4.42 kWh, while iron quartz as the overburden layer of the ore requires 5.70 kWh. The average energy expended is 5.06 kWh. The values of energy expended offer a practical estimate of the energy input needed to grind a given amount of the Anka manganese ore. The obtained value is in line with the range in literature, the results directly influence the development of economical and efficient comminution circuits employed to process Anka manganese ore deposits. When determining comminution energy, the work index alongside the corresponding energy expenditure measurements helps evaluate processing costs and select optimal grinding equipment and operating conditions [16, 17].

Table 5: Particle size analysis of Quartz (Feed into ball mill)

Sieve size range (µm)	Weight retained (g)	% Weight retained	% Cumulative weight retained	% Cumulative weight passing
-1400+1000	64.44	70.23	70.22	29.78
-1000+710	0.23	0.25	70.48	29.52
-710+500	7.85	8.55	79.03	20.97
-500+355	8.47	9.23	88.26	11.74
-355+250	2.78	3.03	91.29	8.71
-250+180	1.89	2.06	93.35	6.65
-180+125	1.80	1.96	95.31	4.69
-125+90	1.37	1.49	96.80	3.20
-90+63	1.96	2.14	98.94	1.06
-63	0.97	1.06	100	0

Table 6: Particle size analysis of quartz (Product from ball mill)

Sieve size range (µm)	Weight retained (g)	% Weight retained	% Cumulative weight retained	% Cumulative weight passing
-1400+1000	1.36	1.40	1.40	98.60
-1000+710	2.42	2.50	3.90	96.10
-710+500	26.14	27.00	30.90	69.10
-500+355	30.36	31.35	62.25	37.75
-355+250	8.71	9.00	71.25	28.75
-250+180	6.73	6.95	78.20	21.80
-180+125	8.23	8.50	86.70	13.30
-125+90	4.31	4.45	91.15	8.85
-90+63	5.31	5.48	96.63	3.37
-63	3.26	3.37	100	0

Table 7: Particle Size Analysis of Iron (Feed into Ball Mill)

Sieve size range (µm)	Weight retained (g)	% Weight retained	% Cumulative weight retained	% Cumulative weight passing
-1400+1000	90.82	90.95	90.95	9.05
-1000+710	0.81	0.81	91.76	8.24
-710+500	1.67	1.67	93.43	6.57
-500+355	1.10	1.10	94.53	5.47
-355+250	0.78	0.78	95.31	4.69

Sieve size range (µm)	Weight retained (g)	% Weight retained	% Cumulative weight retained	% Cumulative weight passing
-250+180	0.87	0.87	96.18	3.82
-180+125	1.24	1.24	97.42	2.58
-125+90	0.80	0.80	98.22	1.78
-90+63	0.73	0.73	98.95	1.05
-63	1.04	1.04	100	0

Table 8: Particle size analysis of Iron (Product from ball mill)

Sieve size range (µm)	Weight retained (g)	% Weight retained	% Cumulative weight retained	% Cumulative weight passing
-1400+1000	0.16	0.17	0.17	99.83
-1000+710	1.53	1.65	1.82	98.18
-710+500	14.72	15.85	17.67	82.33
-500+355	23.71	25.54	43.21	56.79
-355+250	6.02	6.48	49.69	50.31
-250+180	8.64	9.31	59.00	41.00
-180+125	15.94	17.71	76.17	23.83
-125+90	7.9	8.50	84.67	15.33
-90+63	9.97	10.74	95.42	4.58
-63	4.26	4.59	100	0

Table 9: Particle size analysis of Manganese (Feed into ball mill)

Sieve size range (µm)	Weight retained (g)	% Weight retained	% Cumulative weight retained	% Cumulative weight passing
-1400+1000	4.98	5.07	5.07	94.93
-1000+710	0.03	0.03	5.10	94.90
-710+500	15.22	15.51	20.61	79.39
-500+355	16.91	17.23	37.84	62.16
-355+250	7.04	7.17	45.01	54.99
-250+180	4.23	4.31	49.32	50.68
-180+125	10.91	11.12	60.44	39.56
-125+90	13.74	14.00	74.44	25.56
-90+63	14.55	14.83	89.27	10.73
-63	10.53	19.73	100	0

Table 10: Particle size analysis of Manganese (Product from ball mill)

Sieve size range (µm)	Weight retained (g)	% Weight retained	% Cumulative weight retained	% Cumulative weight passing
-1400+1000	0.74	0.40	0.40	99.60
-1000+710	0.15	0.08	0.48	99.52
-710+500	0.66	0.36	0.84	99.16
-500+355	1.81	0.97	1.81	98.19
-355+250	2.18	1.17	2.98	97.02
-250+180	7.32	3.93	6.91	93.09
-180+125	34.59	18.57	25.48	74.52
-125+90	72.63	39.00	64.48	35.52
-90+63	14.52	25.51	89.99	10.01
-63	18.65	10.01	100	0

Using Gaudin Schumann Expression (Equation 2)

Table 11: Sieve mesh size (500 µm and 250 µm) with 80% of particle size passing

Sample	80% Passing of feed product (F80) µm	80% Passing of milled product (P80) µm
Quartz	7214.6	670.5
iron ore	77282	472.5
Anka Manganese	508	144.125

Work index determination (Equation 1)

Table 12: Result of work index and energy expended in grinding

Calculated values	Work index (kWh/ton)	Energy expended in grinding (kWh)
Anka Manganese Ore (quartz)	11.34	4.42
Anka Manganese Ore (iron ore)	14.62	5.70
Average Value Obtained	12.98	5.06

4. CONCLUSION

This study provides a comprehensive characterization of Anka manganese ore, revealing its suitability for industrial beneficiation. The chemical analysis confirmed a high MnO content (52.112%), while mineralogical assessments identified pyrolusite and jacobsite as dominant phases. SEM-EDS analysis highlighted the interlocking nature of manganese, iron, silicon, and aluminium within the ore matrix. Particle size analysis determined the optimal liberation size at -125+90 µm, with a peak MnO concentration of 53.973%. Grindability tests yielded an average work index of 12.98 kWh/ton and an energy expenditure of 5.06 kWh. These results support the development of energy-efficient comminution circuits and underscore the deposit's industrial viability, particularly for steelmaking applications.

ACKNOWLEDGEMENT

The authors wish to appreciate Deutscher Akademischer Austausschdienst (DAAD) for the grant to carry out this research, the Mineral Processing Laboratory of the Department of Metallurgical and Materials Engineering, Federal University of Technology, Akure, Ondo State, Nigeria, and National Steel Raw Materials Exploration Agency, Kaduna for allowing the use of their laboratory equipment during the course of the research.

REFERENCES

[1] Bhaskar, S., Devi, N. B., Rao, D. S., & Raju, G. S. N. (2021). *Manganese ores: Mineralogy, processing, and applications*. CRC Press.
[2] Ding, Y., Li, X., Wang, Y., & Chen, Q. (2022). Recent advances in manganese-based materials for energy storage. *Energy Storage Materials*, 45, 703-731.
[3] United States Geological Survey. (2024). *Mineral commodity summary: Manganese*. U.S. Department of the Interior. Retrieved April 26, 2025, from USGS official website (https://www.usgs.gov)
[4] Norgate, T., & Jahanshahi, S. (2013). Life cycle assessment of metals: From mining to end of life. *Journal of Cleaner Production*, 43, 68-77.
[5] Xun, G., Jiang, Z., Chaolei, B., Xinkuo, L., Guozhao, F., & Shuquan, L., (2020). Zn/MnO2 battery chemistry with dissolution-deposition mechanism, *Materials Today Energy*, 16, 100 - 396
[6] Nwankwo, O., Nwokolo, C., & Okafor, U. (2023). Manganese ore mineralogy and processing: Challenges and prospects in Nigeria. *International Journal of Mineral Processing*, 213, 104-488.
[7] Nigerian Investment Promotion Commission. (2017). *Investment opportunities in the Nigerian mining sector*.
[8] Mishra, D., Murmu, G., & Kumar, S. (2023). Sustainable mining practices: A review. *Environmental Science and Pollution Research*, 30(47), 105156-105175.
[9] Da Silva, F. L. F., Araújo, F. G. S., & Peres, A. E. C. (2018). Beneficiation of manganese ores. *International Journal of Mineral Processing*, 173, 73–89.
[10] Sahoo, S., Sahu, S. N., Ratha, S. S., & Biswal, S. K. (2022). Reducing effect of biomass derived char on iron ore fines; a statistical investigation and regression modelling. *Metallurgical Research & Technology*, 119(4), 417.
[11] Frenzel, M., Ketris, M. P., & Gutzmer, J. (2016). Mineralogical and geochemical characterisation of manganese ores: A review. *Ore Geology Reviews*, 76, 304-361.
[12] Zhang, X., Zhang, Y., & Chen, W. (2024). Mineralogical characterization of low-grade manganese ore for beneficiation. *International Journal of Mineral Processing*, *246*, 107936.
[13] Filippou, D., & Aggelopoulos, C. A. (2016). Manganese ore leaching. In M. J. Nicol & C. A. Fleming (Eds.), *Mineral processing technology*, 395-412.
[14] Free, M. L. (2014). Sieving methods. In P. Worsfold, A. Townshend and C. Poole (Eds.), *Encyclopedia of analytical science*, 3rd ed., 9, 209-216.
[15] Gupta, A., & Yan, D. S. (2016). *Mineral processing design and operation* (1st ed.). Elsevier.

[16] Altun, O., & Benzer, A. H. (2021). Energy efficiency improvement in comminution processes. *Minerals Engineering*, 169, 106 - 962.
[17] Nadolski, S. (2017). Energy efficiency improvement in comminution processes. *Renewable and Sustainable Energy Reviews*, 78, 1137-1147.
[18] Adeoti, M. O., Dahunsi, O. A., Awopetu, O. O., Aramide, F. O., Alabi, O. O., Johnson, O. T., & AbdulKareem,A. S. (2019). Determination of Work Index of Graphite from Saman-Burkono (Nigeria) using Modified Bond's Method. *Nigerian Journal of Technology (NIJOTECH)*, 38(3), 609 – 613.
[19] Wills B.A (2006) Mineral processing technology, 7th edn. Pergamon Press, Oxford.
[20] Gilmour, I. (2016). *An introduction to industrial minerals* (3rd ed.). Elsevier.
[21] Kaplan, H., & Aktas, Z. (2013). Flotation of manganese minerals: A review. *Minerals Engineering*, 52, 7-23.
[22] Littlejohn, C. S., Berry, D. L., & Mlynarczyk, R. E. (2023). *Mineral processing plant design, practice, and control*. SME.
[23] Golden, T. D. (2024). *Lecture 14: X-ray diffraction and figure of merit.* University of North Texas. Retrieved from https://sites.chemistry.unt.edu/~tgolden/course